

Fermi National Accelerator Laboratory

FERMILAB-Conf-94/136-E

CDF

$J/\psi, \psi' \rightarrow \mu^+ \mu^-$  and  $B \rightarrow J/\psi, \psi'$  Cross Sections

The CDF Collaboration

*Fermi National Accelerator Laboratory  
P.O. Box 500, Batavia, Illinois 60510*

June 1994

Submitted to the 27th International Conference on High Energy Physics, Glasgow, Scotland, July 20-27, 1994



## **Disclaimer**

*This report was prepared as an account of work sponsored by an agency of the United States Government. Neither the United States Government nor any agency thereof, nor any of their employees, makes any warranty, express or implied, or assumes any legal liability or responsibility for the accuracy, completeness, or usefulness of any information, apparatus, product, or process disclosed, or represents that its use would not infringe privately owned rights. Reference herein to any specific commercial product, process, or service by trade name, trademark, manufacturer, or otherwise, does not necessarily constitute or imply its endorsement, recommendation, or favoring by the United States Government or any agency thereof. The views and opinions of authors expressed herein do not necessarily state or reflect those of the United States Government or any agency thereof.*

Contribution Code: GLS0208  
Proposed Sessions: Pa-02, Pl-19, Pa-14, Pl-15

CDF/PUB/BOTTOM/PUBLIC/2623  
Fermilab-Conf-94/136-E  
May 27, 1994

# $J/\psi, \psi' \rightarrow \mu^+ \mu^-$ and $B \rightarrow J/\psi, \psi'$ Cross Sections

The CDF Collaboration

Contributed paper to the 27th International Conference on  
High Energy Physics, Glasgow, July 20-27, 1994.

## Abstract

This paper presents a measurement of  $J/\psi, \psi'$  differential cross sections in  $p\bar{p}$  collisions at  $\sqrt{s} = 1.8$  TeV. The cross sections are measured above 4 GeV/c in the central region ( $|\eta| < 0.6$ ) using the dimuon decay channel. The fraction of events from  $B$  decays is measured, and used to calculate  $b$  quark cross sections and direct  $J/\psi, \psi'$  cross sections. The direct cross sections are found to be more than an order of magnitude above theoretical expectations.

## 1 Introduction

Charmonium production is currently the best way to study  $b$  quark production at CDF at the lowest possible transverse momentum of the  $b$ . While the signature and signal-to-noise for the  $J/\psi$  are excellent, the actual conclusions regarding  $b$  production are strongly dependent

Submitted 27th International Conference on High Energy Physics, University of Glasgow, Glasgow, Scotland, July 20-27,<sup>1</sup> 1994

on the fraction of the data sample due to  $b$  decays. One obvious way of determining this fraction is to use the decay distance of the  $J/\psi$  state. In contrast, the fraction of  $\psi'$ 's from  $b$  decays is thought to be close to one[1]. Thus, in determining the  $P_T$  spectrum of  $b$  quarks from a study of  $\psi'$  events, one does not have to worry about the fraction of  $\psi'$  production due to  $B$  decays. In the course of this analysis, however, a very large zero-lifetime component for the observed  $\psi'$  signal has been seen. Therefore, one still has to make use of the lifetime information.

## 2 Detector Description

The CDF detector has been described in detail elsewhere[2]. We describe here briefly the components relevant to this analysis. The CDF coordinate system defines the beam line to be the  $z$  direction.  $R$  is the radial distance from the beam line, and  $\phi$  is the azimuthal angle. A solenoidal magnet generating a 1.4 T magnetic field surrounds the two tracking chambers used. The Central Tracking Chamber (CTC) is a cylindrical drift chamber surrounding the beam line.

The CTC contains 84 layers, which are grouped into nine superlayers, with 5 superlayers providing axial information and 4 providing stereo. It covers a pseudorapidity range of  $|\eta| < 1.1$ . The Silicon Vertex Detector (SVX) is a silicon microvertex detector. It consists of four layers 2.9 to 7.9 cm from the beam line and provides high resolution tracking information in the  $R - \phi$  plane. When combined with a CTC track, it provides an impact parameter resolution of  $(13 + 40/P_T)\mu\text{m}$  and a transverse momentum resolution of  $\sqrt{(0.0009P_T)^2 + (0.0066)^2}$ . Primary vertices have a Gaussian distribution with a width of about 27 cm, while the SVX only reaches to  $\pm 25\text{cm}$ , so only about 60% of the CTC tracks can be augmented with SVX information.

Outside the CTC are electromagnetic and hadronic calorimeters, which provide five absorption lengths of material before the Central Muon Chambers (CMU). The CMU consists of four layers of limited streamer chambers. It is divided into 72 segments which cover 85% of the  $\phi$  region for  $|\eta| < 0.6$ . Muons with  $P_T$  below  $\sim 1.4 \text{ GeV}/c$  range out in the calorimeters.

The CDF trigger consists of three levels. In the first level, both muons must be detected in the CMU. They must be separated by at least 0.09 radians in  $\phi$  and pass a slope cut in the  $R - \phi$  plane. The slope cut is effectively a cut on the transverse momentum. To pass the second level, a fast hardware tracker must find at least one track that points to the correct muon chamber. For the third level, the full CTC track reconstruction is done. Both tracks must be found, and extrapolate to within  $4\sigma$  of the muon chamber tracks in  $R - z$  and  $R - \phi$ .  $\sigma$  is the expected multiple scattering error added in quadrature with the measurement error.

## 3 Event Selection

Further cuts are applied offline to produce a purer sample. The CTC track and the CMU segment are required to match better than  $3\sigma$  in  $R - \phi$ , and  $3.5\sigma$  for the  $J/\psi$  and  $3\sigma$  for

the  $\psi'$  in  $R - z$ . Hadronic energy is required in the calorimetry tower that points to the muon chambers in the  $\psi'$  events. Both muons are required to have  $P_T^\mu > 2.0$  GeV/ $c$  and one muon must have  $P_T^\mu > 2.8$  GeV/ $c$ . The dimuon is required to have  $|\eta^{\mu\mu}| < 0.6$  and  $P_T^{\mu\mu} > 4$  GeV/ $c$ . Runs with known hardware problems were excluded. Because there are much better statistics in the  $J/\psi$ , a tighter definition of bad runs was used there, resulting in a smaller integrated luminosity.

For the  $J/\psi$ , the CTC track is beam constrained. In the  $\psi'$ , the tracks are vertex constrained, using the SVX information if there are three or more hits. The  $\chi^2$  of this fit is required to be less than 10, with one degree of freedom. The resulting invariant mass is used to define a signal region of  $3.0441 < m_{\mu\mu} < 3.1443$  GeV/ $c^2$  for the  $J/\psi$  and  $3.636 < m_{\mu\mu} < 3.736$  GeV/ $c^2$  for the  $\psi'$ . Sideband regions of  $2.9606 < m_{\mu\mu} < 3.0274$  GeV/ $c^2$  or  $3.1610 < m_{\mu\mu} < 3.2278$  GeV/ $c^2$  for the  $J/\psi$  and of  $3.52 < m_{\mu\mu} < 3.62$  GeV/ $c^2$  or  $3.75 < m_{\mu\mu} < 3.85$  GeV/ $c^2$  for the  $\psi'$  are also defined.

Figure 1 show the mass distribution of the events passing these cuts. There are a total of  $26533 \pm 175$   $J/\psi$  events and  $896 \pm 94$   $\psi'$  events.

## 4 B Fraction

For events where both muons have SVX tracks with at least three hits, we vertex constrain the tracks to measure  $l_{xy}$ , the projection of the decay length onto the  $J/\psi, \psi'$  transverse momentum. This is converted into the proper lifetime of the parent by  $c\tau = l_{xy}/[(P_T/m) \cdot F^{corr}]$ , where  $F^{corr}$  is a Monte Carlo correction factor that relates the  $J/\psi, \psi'$  transverse momentum to the transverse momentum of the parent.

The background  $c\tau$  shape is measured from the sidebands. It contains non-Gaussian tails, so we parametrize it by

$$B(x) = \begin{cases} (1 - f_+ - f_-) \frac{1}{\sqrt{2\pi}\sigma} \exp\left(-\frac{x^2}{2\sigma^2}\right) + f_+ \cdot \frac{1}{\lambda_+} \exp\left(\frac{-x}{\lambda_+}\right) & , x > 0 \\ (1 - f_+ - f_-) \frac{1}{\sqrt{2\pi}\sigma} \exp\left(-\frac{x^2}{2\sigma^2}\right) + f_- \cdot \frac{1}{\lambda_-} \exp\left(\frac{x}{\lambda_-}\right) & , x \leq 0 \end{cases}$$

where  $f_+$  is the fraction in the positive exponential,  $\lambda_+$  is the lifetime of the positive exponential,  $f_-$  is the fraction in the negative exponential,  $\lambda_-$  is the lifetime of the negative exponential, and  $\sigma$  is the width of the central Gaussian. The signal region is the fit to the function  $N \cdot f_{sig}(c\tau)$ , where

$$f_{sig}(c\tau) = f_{back} \cdot B(c\tau) + (1 - f_{back}) [(1 - f_B) \cdot R(c\tau) + f_B \cdot R \star E(c\tau)]$$

where  $R(c\tau) = f_r \frac{1}{\sqrt{2\pi}\sigma} \exp\left(-\frac{c\tau^2}{2\sigma^2}\right) + (1 - f_r) \frac{1}{\lambda} \exp\left(\frac{-|c\tau|}{\lambda}\right)$  is the resolution function and  $E(c\tau) = \frac{1}{c\tau_0} \exp\left(\frac{-c\tau}{c\tau_0}\right)$ .  $f_{back}$  is the background fraction,  $f_B$  is the B fraction,  $c\tau_0$  is the B lifetime,  $\sigma$  is the width of the Gaussian,  $f_r$  is the fraction of non-Gaussian tails in resolution function, and  $\lambda$  is the lifetime of non-Gaussian tails.  $R \star E(c\tau)$  is the convolution of the resolution function with an exponential. We fix  $c\tau_0$  to 438  $\mu\text{m}$ , as found by the CDF inclusive

$B$  lifetime measurement.[4].  $f_{back}$  is calculated by

$$f_{back} = \frac{\Delta m(\text{Signal})}{\Delta m(\text{Sideband})} \cdot \frac{N_{\text{Sideband}}^{\text{Entries}}}{N_{\text{Signal}}^{\text{Entries}}} = \frac{N_{\text{Sideband}}^{\text{Entries}}}{2 \cdot N_{\text{Signal}}^{\text{Entries}}}.$$

In the  $\psi'$  the data is fit using an unbinned log-likelihood fit.  $f_{back}$  is not fixed, but a Poisson term is included for the likelihood that the fitted value fluctuates to the calculated value.  $\sigma$  is calculated on an event by event basis. Using the event-by-event error introduces non-Gaussian tails into the total resolution function, so  $f_r$  is fixed at 1. The systematic error is estimated in part by allowing  $f_r$  and  $\lambda$  to be fitted. In the  $J/\psi$ , the signal and sidebands are fit in separate binned fits.  $f_{back}$  is fixed and  $\sigma$ ,  $f_r$  and  $\lambda$  are fit. Figure 2 show the result of the fits.

## 4.1 $P_T$ dependence

It is expected that the  $B$  fraction in the  $J/\psi, \psi'$  samples rises with  $P_T$ . To measure this, we divide the  $\psi'$  sample into three  $P_T$  bins from 4 – 6 GeV, 6 – 9 GeV, and 9 – 20 GeV. The size of the last bin is necessitated by the low statistics at high  $P_T$ . We then repeat the above fitting procedure in each of the  $P_T$  regions.

In the  $J/\psi$  sample, the “spectrum method” is used to calculate the  $P_T$  dependence. This is done in three steps. First, the  $J/\psi$   $P_T$  spectrum is obtained. Then, the spectrum of events with  $c\tau > 250\mu\text{m}$  is found. The two are normalized so that the ratio of the total area is the inclusive  $B$  fraction found above. The  $B$  fraction is then obtained by dividing the two distributions. The results are shown in Tables 1 and 2.

## 5 Acceptance and Efficiencies

The  $J/\psi, \psi'$  differential cross section is defined by

$$\frac{d\sigma}{dP_T}(P_T) = \frac{N}{\alpha \cdot \epsilon \cdot \int \mathcal{L} dt \cdot \Delta P_T}$$

where  $N$  is number of  $J/\psi, \psi'$  candidates in the bin,  $\alpha$  is the detector and kinematic acceptance,  $\epsilon$  is the trigger and cut efficiency,  $\int \mathcal{L} dt$  is the integrated luminosity, and  $\Delta P_T$  is the size of the  $P_T$  bin. The acceptance was determined from several Monte Carlo data sets. The  $\psi'$  acceptance used  $\psi'$ 's generated flat in  $P_T$  and  $\eta$ . The  $J/\psi$  acceptance used several sets where  $b$  quarks were generated in different  $P_T$  ranges, in order to provide sufficient statistics in all regions. The  $b$  quarks were generated using the next-to-leading order QCD calculation[3] and MRSD0 structure functions. The quarks were fragmented to  $B$  mesons using Peterson fragmentation[9] with  $\epsilon_b = 0.006 \pm 0.002$ . A fast detector simulation was used on the events, and the kinematic cuts were then applied to the events. The  $J/\psi, \psi'$  acceptance is the ratio of events that survived this process to the number of generated events.

$P_T$ (GeV/ $c$ )	B Fraction (%)
Above 4	$19.6 \pm 1.5$
4 – 5	$13.3 \pm 1.0$
5 – 6	$15.9 \pm 1.2$
6 – 7	$21.0 \pm 1.7$
7 – 8	$25.2 \pm 2.1$
8 – 9	$25.2 \pm 2.2$
9 – 10	$26.9 \pm 2.5$
10 – 11	$34.3 \pm 3.3$
11 – 12	$31.0 \pm 3.5$
12 – 13	$32.4 \pm 4.1$
13 – 14	$42.1 \pm 5.7$
14 – 15	$27.6 \pm 5.0$

Table 1: Differential  $B$  fraction and cross section (from all sources) of  $J/\psi$ . Errors are statistical plus systematic.

$P_T$ (GeV/ $c$ )	B Fraction (%)
Above 4	$22.8 \pm 3.8$
4 – 6	$12.3 \pm 4.9$
6 – 9	$29.5 \pm 7.0$
9 – 20	$39.3 \pm 7.9$

Table 2: Differential  $B$  fraction and cross section (from all sources) of  $\psi'$ . Errors are statistical plus systematic.

The  $b \rightarrow J/\psi, \psi'$  acceptance used events where  $b$  quarks were generated and forced to decay to  $J/\psi, \psi'$ . The  $J/\psi, \psi'$  was forced to have the momentum spectrum measured by [5],[6]. The  $P_T$  of the  $b$  quark is described by  $P_T^{min}$ .  $P_T^{min}$  is defined as the  $P_T$  such that about 90% of the  $b$  quarks in our sample have  $P_T^b > P_T^{min}$ . The  $b$  quark acceptance is then calculated by

$$\alpha_b = \frac{N_b(P_T^{J/\psi, \psi'} > 4.0 \text{ GeV}/c, |\eta^{J/\psi, \psi'}| < 0.6, |y^b| < 1.0)}{N_b(P_T^b > P_T^{min}, |y^b| < 1.0)}$$

The lack of a  $P_T$  cut on the  $b$  in the numerator corrects for the fact that we are unable to remove those events with  $P_T^b < P_T^{min}$ .

The efficiencies of the three triggers were studied with unbiased  $J/\psi$  events, as were the muon quality cuts. The efficiency of the CTC track reconstruction is  $98.9 \pm 1.0\%$ . The efficiency of the muon reconstruction is  $98 \pm 1\%$ .

## 6 Systematics

Systematic errors can arise in three distinct areas: measuring the  $J/\psi, \psi'$  cross sections, determining what portion of that cross section is from  $B$  decays, and extrapolating those results to a  $b$  quark cross section.

### 6.1 $J/\psi, \psi'$ Cross Section Systematics

We calculate the uncertainty due to the trigger efficiency shape by varying the shape of the level 1 and level 2 trigger efficiency parametrizations. This is an 8% effect in the  $J/\psi$  and a 6.6% effect in the  $\psi'$ . We estimate the effect of the acceptance correction in the  $\psi'$  by varying the acceptance by the statistical error and by fitting the acceptance to a fifth degree polynomial, which is a 3.1% effect. In the  $J/\psi$ , fits to different order polynomials were used, giving a 1.5% error. A 5% error is assigned due to the  $J/\psi, \psi'$  polarization based on a  $\sim 10\%$  difference between the acceptance of maximally polarized  $J/\psi$ 's with extreme values of  $\alpha = \pm 1$ . The 1% error measuring the cut efficiencies is negligible compared to other errors. There is a 2% error associated with each of the level 3 trigger efficiency, the CTC tracking efficiency, and the muon reconstruction efficiency. We assign a 4% systematic to the uncertainty in the luminosity.

### 6.2 $B$ Fraction Systematics

Potential sources of systematic errors arise from the  $B$  lifetime, the spread of the  $\sigma_{c\tau}$  distribution, and the fitting technique.

A single value for the  $c\tau$  resolution is assumed in the  $J/\psi$  fit, while a wide range exists. The effect of this is estimated by applying a cut of  $\sigma_{c\tau} < 60\mu\text{m}$ , which removes the long tail in the distribution.  $\sigma_{c\tau}$  is related to the opening angle between the muons, which decreases

at higher  $P_T$ . Since the  $J/\psi$  from  $B$  decays have a harder  $P_T$  spectrum, this may bias the  $B$  fraction, which is lower with this cut. The 7% difference is used as the systematic error. In the  $\psi'$ , the unbinned fit uses the event-by-event error, so this effect is missing. Varying the  $B$  lifetime by one sigma changes the  $B$  fraction by 0.002 or less. This is negligible compared to other contributions.

Changing the fitting technique and the form of the fitted function in the  $\psi'$  can change the  $B$  fraction by 7%, which is used as the systematic error.

### 6.3 B Cross Section Systematics

We assign a 1.3% systematic error due to the uncertainty in the rapidity spectrum in the range  $0.6 < |y^b| < 1.0$ . We take an uncertainty of 4.6% due to the uncertainty in the NDE spectrum with different values of  $\mu$  and  $\Lambda$ . We assign 5% based on half the difference in the acceptance calculated with Peterson epsilon set to 0.004 and 0.008. A systematic of 5% is assigned based on the uncertainty in the CLEO  $J/\psi, \psi'$  momentum distribution. We assign a 1% error because of the statistics in the b to  $\psi'$  Monte Carlo.

In the  $\psi'$ , the effect of the large bin sizes for  $f_B$  is estimated by fitting the B-fraction to a straight line, and using a bin-by-bin correction factor.

## 7 Cross Section

### 7.1 $J/\psi, \psi'$ Cross Section

The cross sections are shown in Figure 3. The integrated cross sections are

$$\sigma(p\bar{p} \rightarrow J/\psi, P_T^{J/\psi} < 4 \text{ GeV}/c, |\eta| < 0.6) \cdot Br(J/\psi \rightarrow \mu^+ \mu^-) = \\ 29.10 \pm 0.19(stat) \pm_{-2.84}^{+3.05}(syst) \text{ nb}$$

$$\sigma(p\bar{p} \rightarrow \psi', P_T^{\psi'} < 4 \text{ GeV}/c, |\eta| < 0.6) \cdot Br(\psi' \rightarrow \mu^+ \mu^-) = \\ 0.721 \pm 0.058(stat) \pm 0.072(syst) \text{ nb}$$

The cross section from  $B$  decays is extracted by multiplying the differential  $B$  fraction by the cross section. We can also obtain a prompt cross section by multiplying the cross section by one minus the  $B$  fraction. The results are shown in Figures 3 and 4. The prompt theory curves are from [11].

### 7.2 Inclusive $b$ Cross Section

We now convert these cross sections into an inclusive  $b$  cross section. We do so using the standard formula,

$$\sigma(p\bar{p} \rightarrow bX, |\eta^b| < 1.0, P_T^b > P_T^{min}) =$$

$$\frac{1}{2} \frac{1}{\int \mathcal{L} dt \cdot \alpha_b} \frac{1}{Br(b \rightarrow J/\psi, \psi' X) \cdot Br(J/\psi, \psi' \rightarrow \mu\mu)} \left( \sum_{P_T} \frac{N(P_T)}{\alpha(P_T) \cdot \epsilon(P_T)} \right)$$

The factor of  $\frac{1}{2}$  results from the fact that the  $b$  or the  $\bar{b}$  can decay into the  $J/\psi, \psi'$ . We use branching ratios of  $Br(b \rightarrow J/\psi X) = 1.16 \pm 0.09\%$  [7],  $Br(b \rightarrow \psi' X) = 0.30 \pm 0.06\%$  [6],  $Br(J/\psi \rightarrow \mu\mu) = 6.27 \pm 0.20\%$  [8] and  $Br(\psi' \rightarrow \mu\mu) = 0.88 \pm 0.13\%$  [10]. Our results are

$$\sigma(p\bar{p} \rightarrow bX, |y^b| < 1.0, P_T^b > 6.0 \text{ GeV}/c) = 12.16 \pm 2.07 \mu\text{b} \quad J/\psi$$

$$\sigma(p\bar{p} \rightarrow bX, |y^b| < 1.0, P_T^b > 7.3 \text{ GeV}/c) = 8.24 \pm 1.34 \mu\text{b} \quad J/\psi$$

$$\sigma(p\bar{p} \rightarrow bX, |y^b| < 1.0, P_T^b > 8.7 \text{ GeV}/c) = 5.20 \pm 0.83 \mu\text{b} \quad J/\psi$$

$$\sigma(p\bar{p} \rightarrow bX, |y^b| < 1.0, P_T^b > 5.9 \text{ GeV}/c) = 6.12 \pm 2.04 \mu\text{b} \quad \psi'$$

$$\sigma(p\bar{p} \rightarrow bX, |y^b| < 1.0, P_T^b > 8.3 \text{ GeV}/c) = 3.85 \pm 1.23 \mu\text{b} \quad \psi'$$

The error is statistical and systematic errors, added in quadrature.

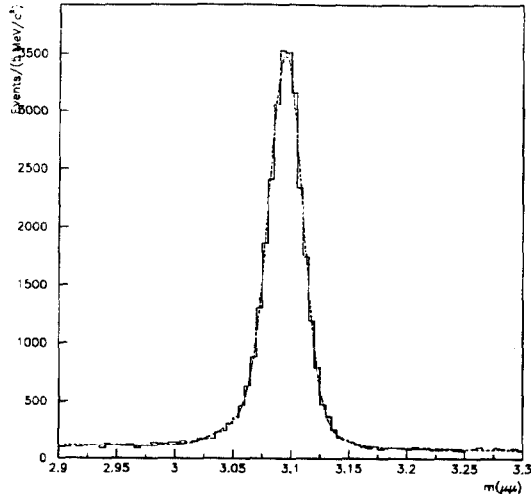
## 8 Acknowledgements

We thank the Fermilab staff and the technical staffs of the participating institutions for their vital contributions. This work was supported by the U.S. Department of Energy and National Science Foundation; the Italian Istituto Nazionale di Fisica Nucleare; the Ministry of Education, Science and Culture of Japan; the Natural Sciences and Engineering Research Council of Canada; the National Science Council of the Republic of China; the A. P. Sloan Foundation; and the Alexander von Humboldt-Stiftung.

## References

- [1] S.D. Ellis, *et al.*, *Phys. Rev. Lett.* **36**, 1263 (1976); C.E. Carlson and R. Suaya, *Phys. Rev. D* **15**, 1416 (1977)
- [2] F.Abe *et al.*, CDF Collab., *Nucl. Instrum. Methods Phys. Res., Sect. A*, **271**, 387 (1988)
- [3] P. Nason *et al.*, *Nucl. Phys.* **B327** 49 (1988)
- [4] F. Abe *et al.*, *Published Proceedings Advanced Study Conference On Heavy Flavours*, Pavia, Italy, September 3-7, 1993. FERMILAB-CONF-93/319-E
- [5] W. Chen, *Decays of Upsilon Mesons to the  $J/\psi$  Meson and a Search for the Higgs Boson in B Meson Decay*, Purdue University Thesis, May 1990
- [6] T. Browder *et al.*, "A Review of Hadronic and Rare B Decays", To appear in *B Decays*, 2nd edition, Ed. by S. Stone, World Scientific
- [7] Y. Kubota *et al.*, "Inclusive Decays of B Mesons to  $J/\psi$  and  $\psi'$ ," Contributed paper at XVI International Symposium on Lepton-Photon Interactions: Cornell University, Ithaca, N.Y., U.S.A., August 10-15, 1993
- [8] Particle Data Group, M.Aguillar-Benitez *et al.*, *Phys. Rev.* **D45**, (1992)
- [9] C. Peterson *et al.*, *Phys. Rev. D*, **27**, 105 (1983)
- [10] G.J. Feldman and M.L. Perl, *Physics Letters*, **33C**, 285 (1977)
- [11] E. Braaten *et al.*, Fermilab Preprint, FERMILAB-PUB-94/135-T (1994)

CDF Preliminary



CDF Preliminary

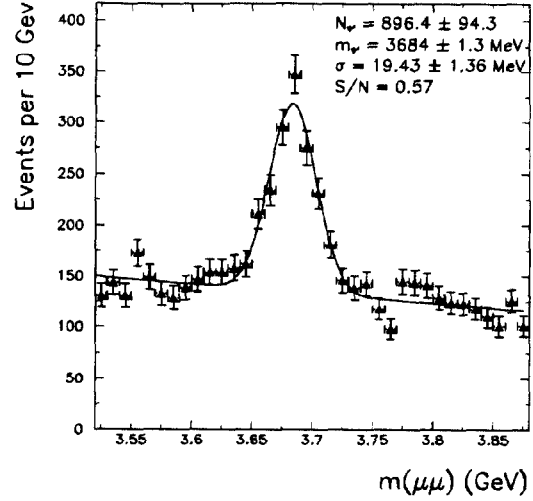


Figure 1: Mass distribution ( $J/\psi$ ,  $\psi'$ )

CDF Preliminary

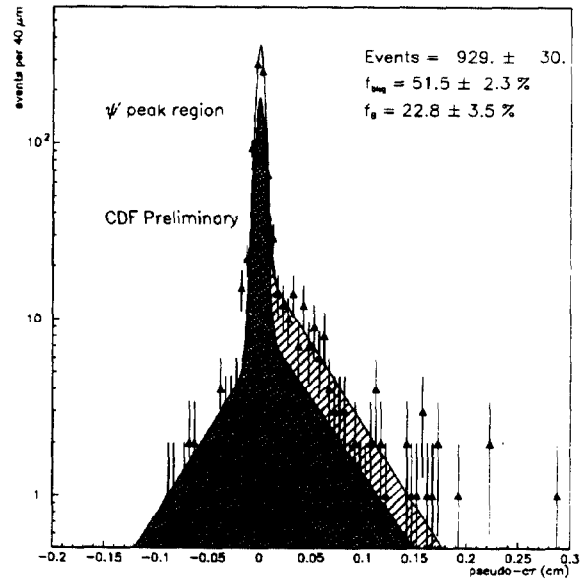
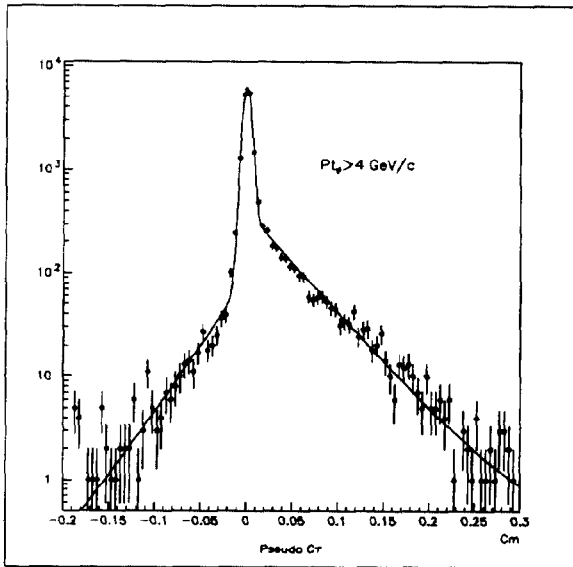


Figure 2:  $J/\psi$  and  $\psi'$  Lifetime Distributions. In the  $\psi'$  plot, the dark region is the background shape. The slashed region is the B component, plus the background shape. The clear region shows a clear excess of prompt events.

CDF Preliminary

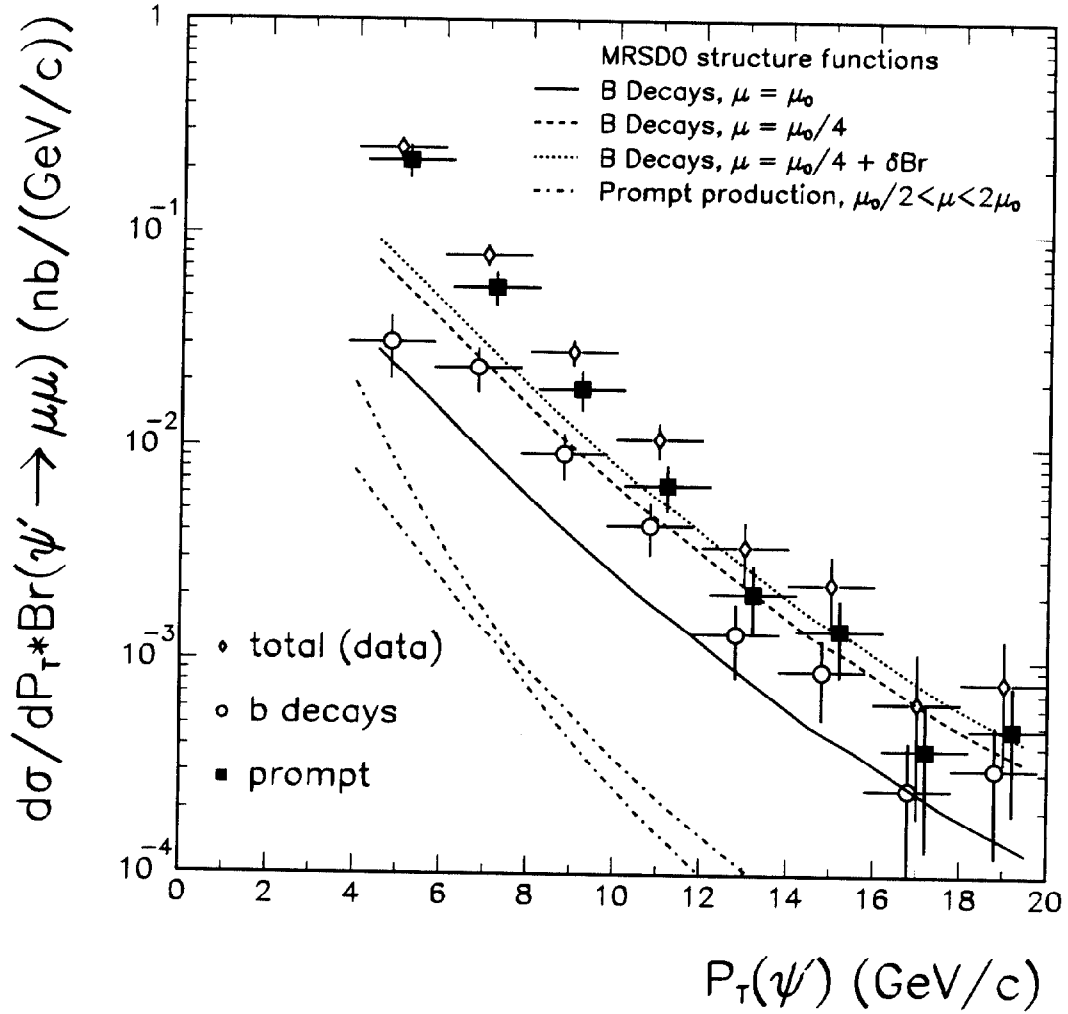


Figure 3:  $\psi'$  Differential Cross Sections. The B(prompt) values have been artificially offset by 200(-200) MeV/c for clarity.

CDF PRELIMINARY

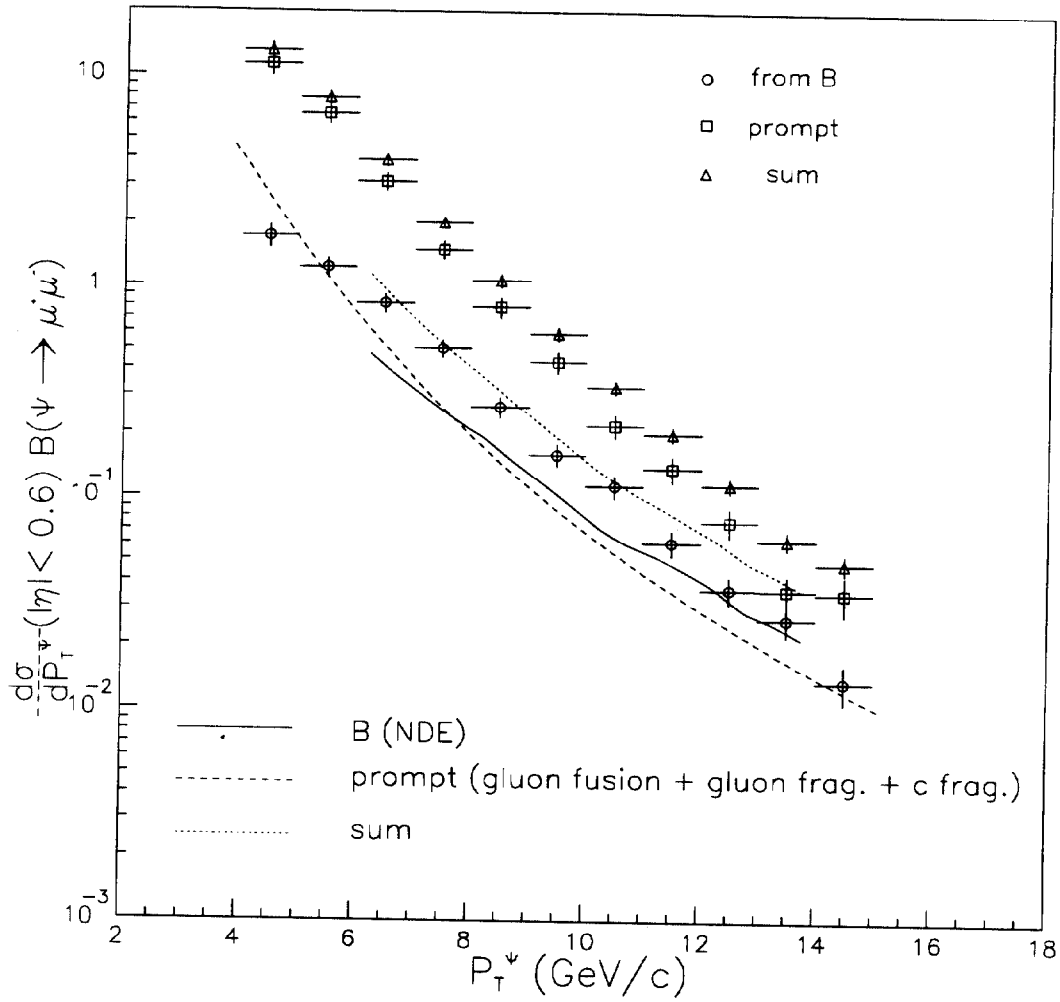


Figure 4:  $J/\psi$  Differential Cross Sections

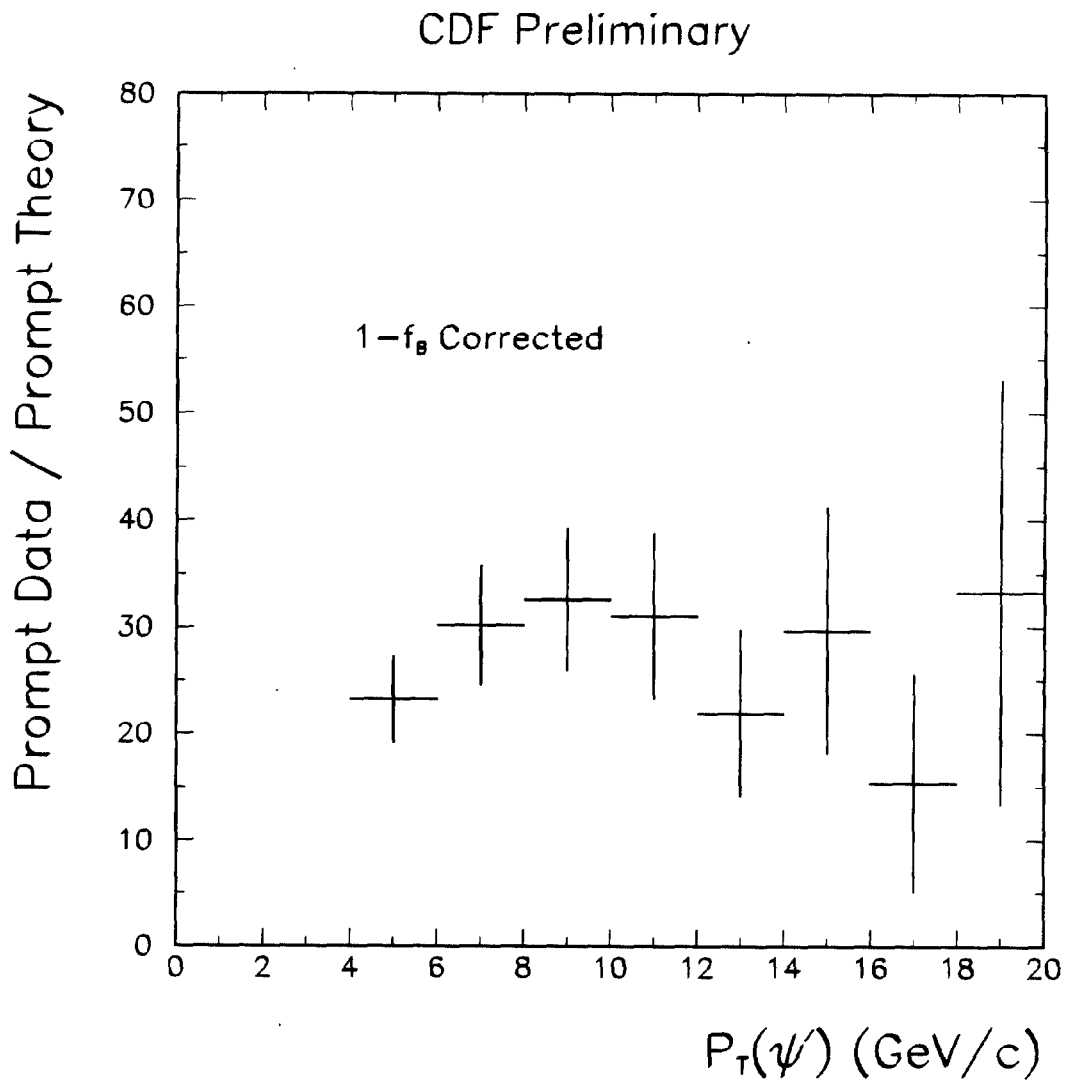


Figure 5: Ratio of data to theory for non-B  $\psi'$  Cross Section